Electronic Supplementary Information (ESI) for

Large-scale facile synthesis of Fe-doped SnO$_2$ porous hierarchical nanostructures and their enhanced lithium storage properties

Yuan Yan, [a] **Feihu Du,** [b] **Xiaoping Shen,** [a,*] **Zhenyuan Ji,** [a] **Hu Zhou,** [c] **Xuexi Sheng** [a] **and Guoxing Zhu** [a]

[a] *School of Chemistry and Chemical Engineering, Jiangsu University, Zhenjiang 212013, P. R. China*
[b] *School of Chemistry and Chemical Engineering, Shanghai Jiao Tong University, Shanghai 200240, P. R. China.*
[c] *School of Material Science and Engineering, Jiangsu University of Science and Technology, Zhenjiang 212003, P. R. China*

*Corresponding author. E-mail: xiaopingshen@163.com

Table S1. Precursors of Sn$_m$[Fe(CN)$_6$]$_n$ obtained with different conditions.

Initial feeding amount of SnCl$_2$ (mmol)	Initial feeding amount of K$_3$Fe(CN)$_6$ (mmol)	* Sn/Fe molar ratio
3	2	2.09
6	2	2.55
9	2	2.88

* The Sn/Fe molar ratios in the Sn$_m$[Fe(CN)$_6$]$_n$ samples were determined by EDX.
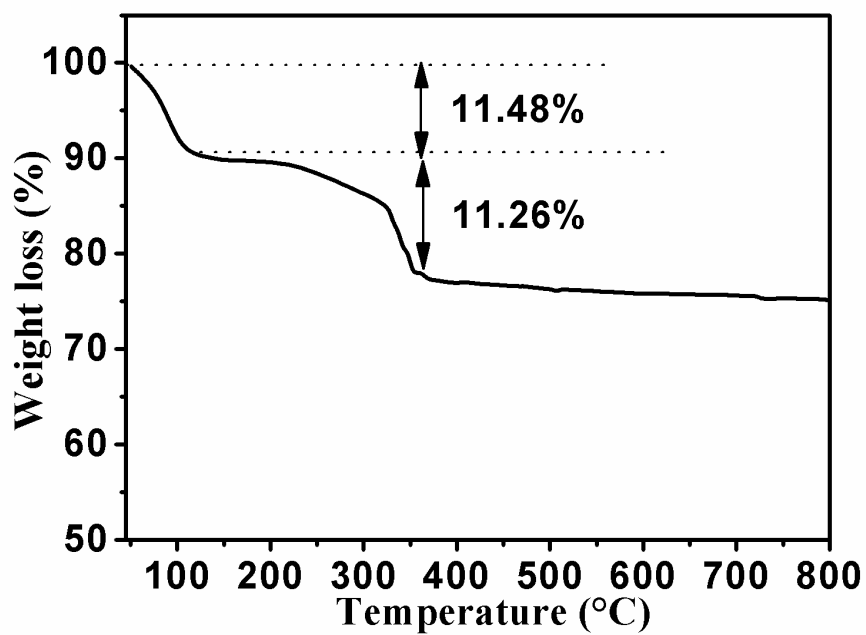
Fig. S1 TGA curve of $Sn_m[Fe(CN)_6]_n$ precursor with a heating rate of 10 °C min^{-1}.
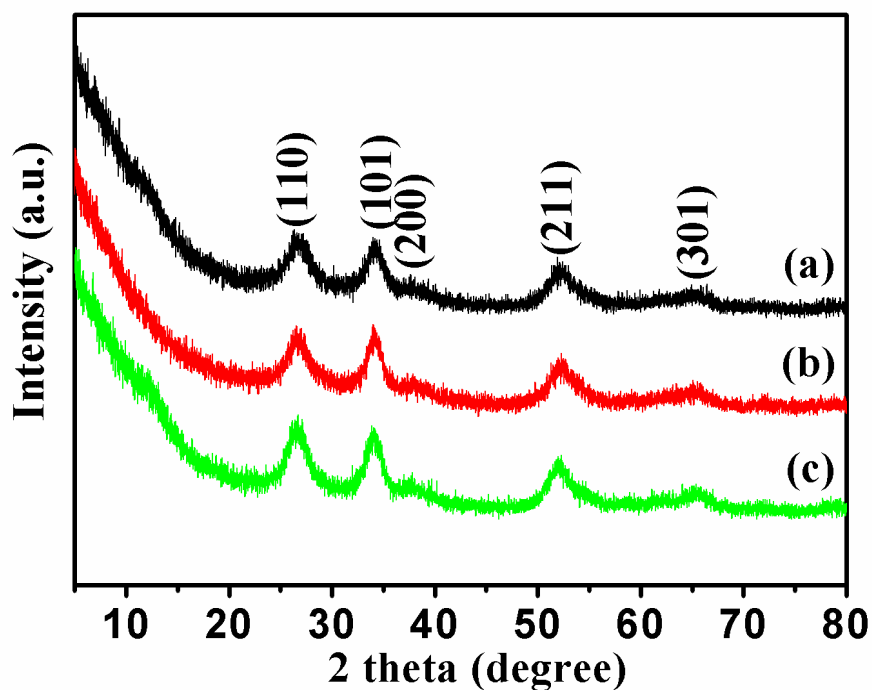

Fig. S2 XRD patterns of (a) SF1-350, (b) SF2-350 and (c) SF3-350.
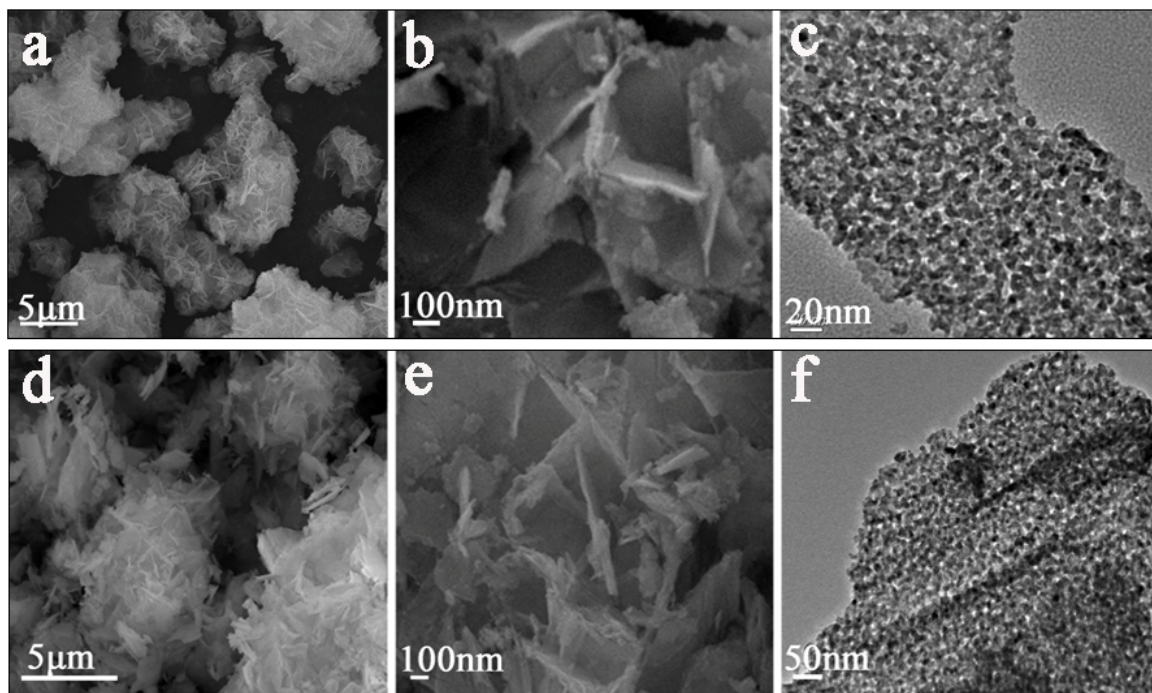
Fig. S3 FESEM and TEM images of (a-c) SF1-450 and (d-f) SF1-650.
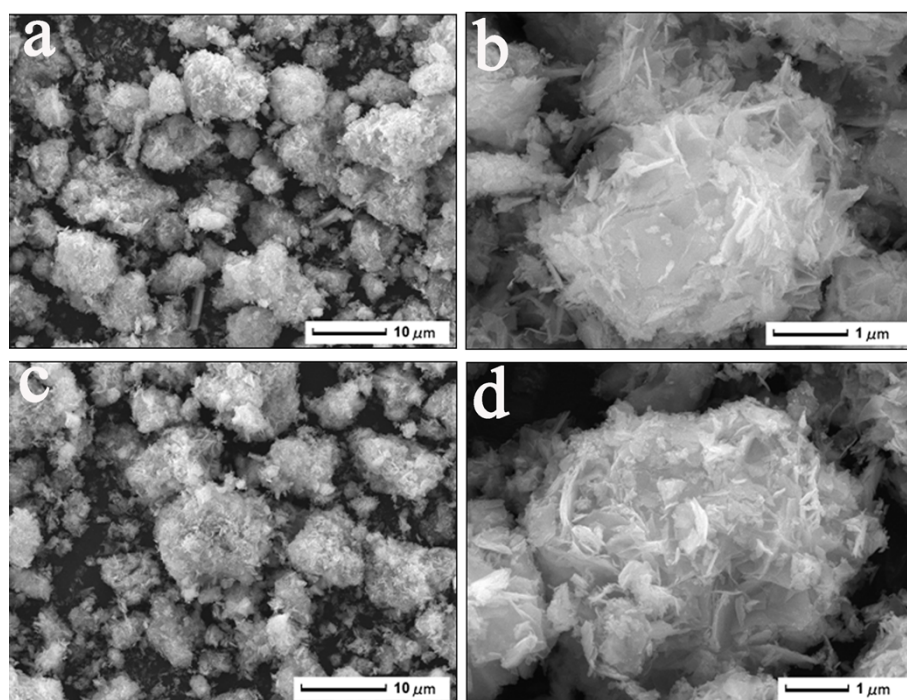

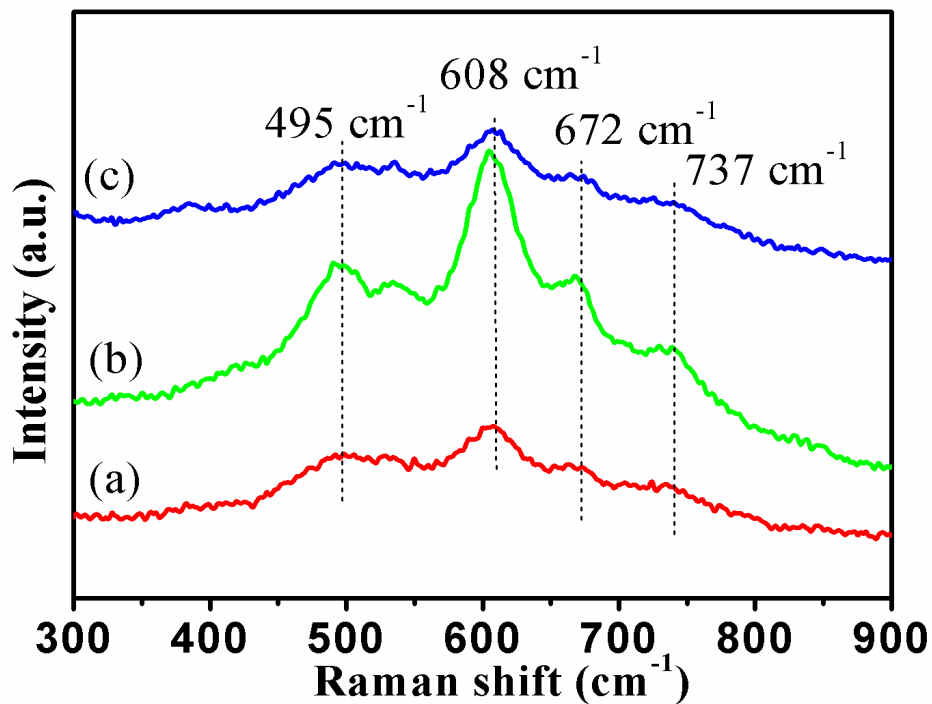**Fig. S4** FESEM images of (a-c) SF2-350 and (d-f) SF3-350.

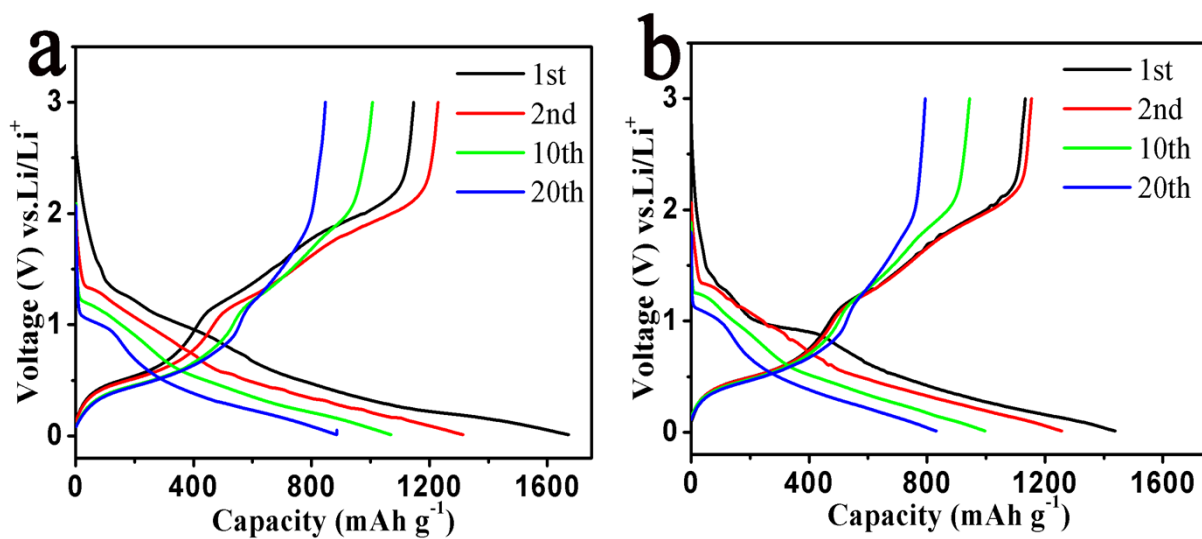**Fig. S5** Raman spectra of (a) SF1-350, (b) SF1-450 and (c) SF1-650.

Fig. S6 Galvanostatic discharge/charge profiles of SF1-450 (a) and SF1-650 (b) at 200 mA g^{-1}.
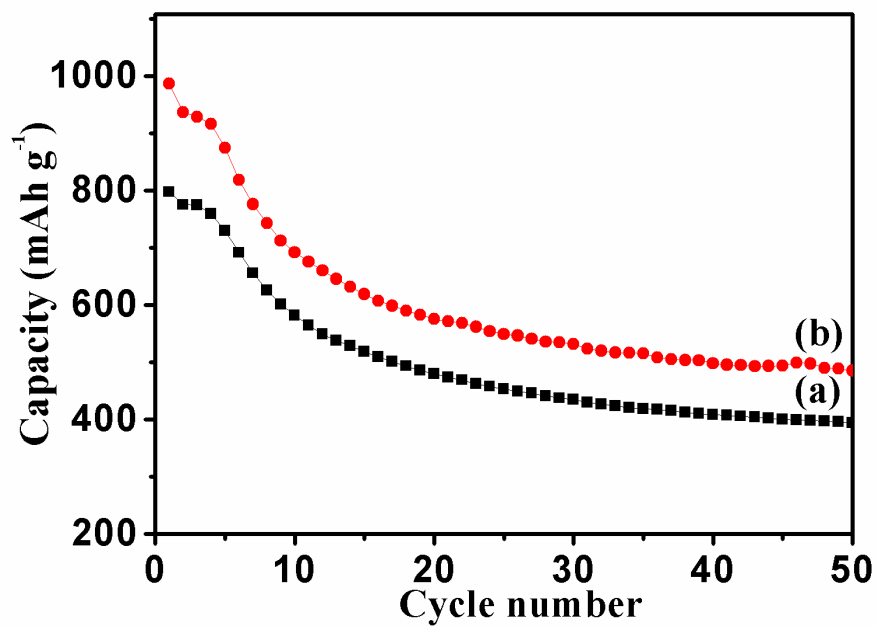
Fig. S7 Lithium storage properties of (a) SF2-350 and (b) SF3-350 at 200 mA g^{-1}.
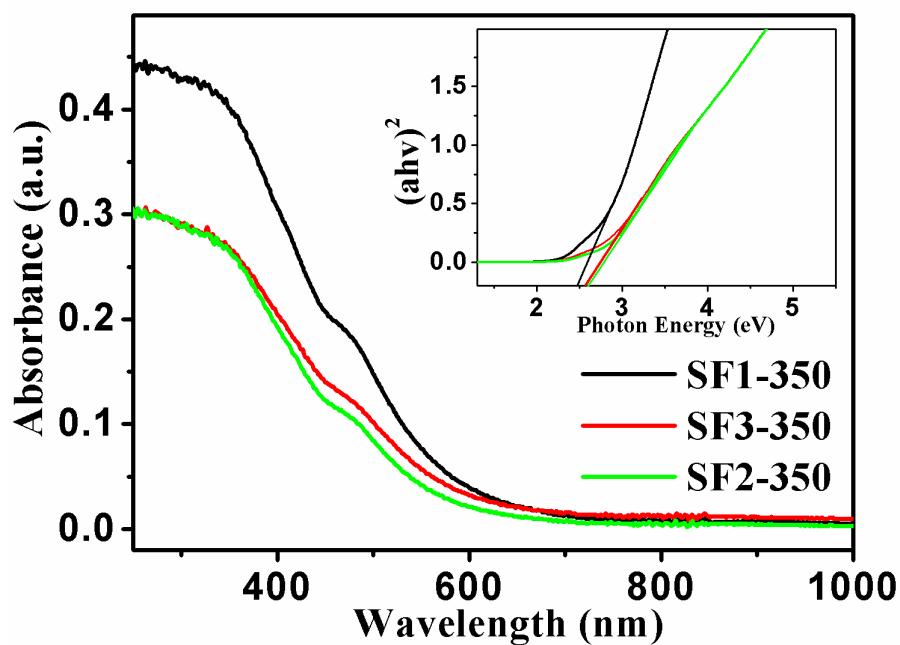

Fig. S8 UV-vis spectra of SF1-350, SF2-350, and SF3-350. Inset shows (ahv)^2 *vs.* photon energy plots of SF1-350, SF2-350 and SF3-350.
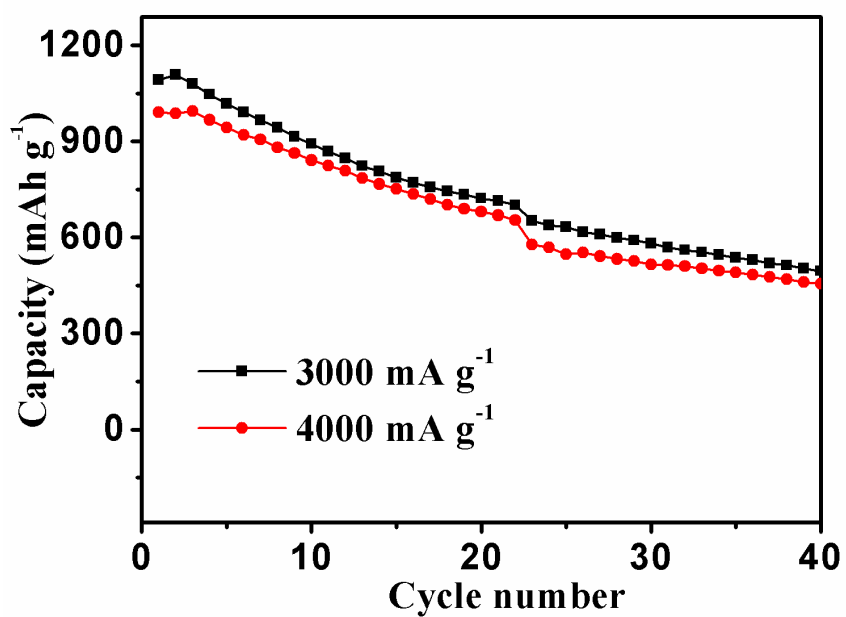
Fig. S9 Lithium storage properties of SF1-350 at the current density of 3000 and 4000
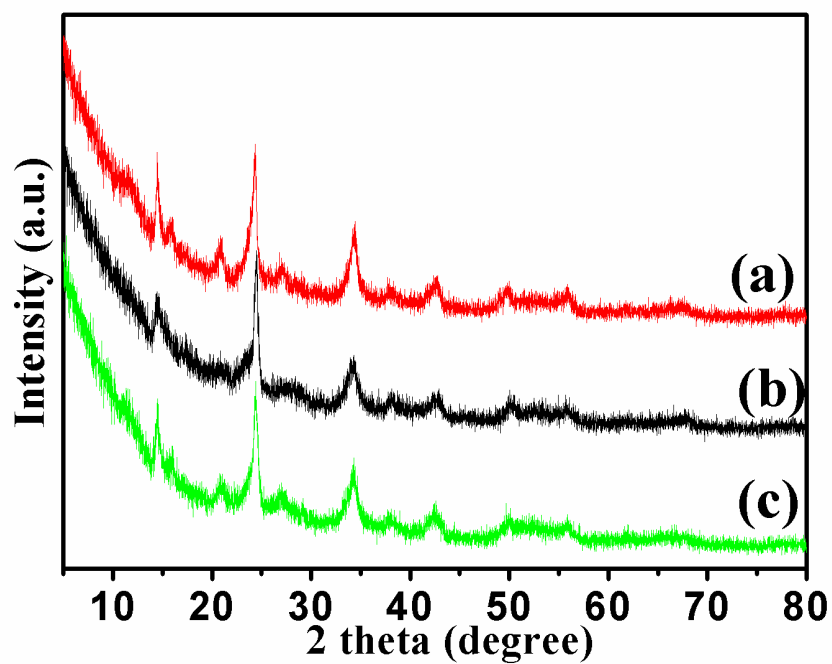
mA g^{-1}, respectively.

Fig. S10 XRD patterns of $Sn_m[Fe(CN)_6]_n$ (a) Sn/Fe=2.55; (b) Sn/Fe=2.09; (c)

Sn/Fe=2.88